Surface Science 272 (1992) 94–101
North-Holland

surface science

Adsorption induced reconstruction of the Cu(110) surface

W. Moritz, R. Zuschke, S. Pflanz, J. Wever and D. Wolf
Institut für Kristallographie und Mineralogie, Universität München, Theresienstrasse 41, D-8000 München 2, Germany

Received 3 December 1991; accepted for publication 19 December 1991

The formation of the O/Cu(110)-(2 × 1) and H/Cu(110)-(1 × 2) superstructures has been investigated by a LEED beam profile analysis. The oxygen induced reconstruction proceeds at later stages by creation of holes on flat terraces. This could not be observed at the hydrogen induced missing row reconstruction. The formation of the missing row structure proceeds most probably via nucleation at steps and subsequent growth of (1 × 2) islands. The influence of different distributions of steps and islands on beam profiles is discussed.

1. Introduction

In a number of cases adsorption on metal surfaces causes a complete restructuring of one or more of the top substrate layers. This process requires the diffusion of substrate atoms over distances which are large compared to the size of the unit cell and are comparable to the size of the terraces. It is evident that by the reconstruction the morphology of the surface will be changed. That means, the mean terrace sizes, the size distribution and in certain cases also the step height distribution of the reconstructed surface will differ from that of the initial clean surface. It is also well known that in many cases adsorbate induced facetting occurs which might be due to the creation of large holes at dislocations or due to an anisotropy of the free energy of the adsorbate covered surface.

The change of the morphology can be observed by diffraction methods. The beam profile analysis provides an easily accessible information about the step distribution and the growth of reconstructed areas. The direct image of the STM, of course, provides the most convincing observation of the local arrangement of defects at surfaces and shows details which cannot be determined from the diffraction pattern. The diffraction method, on the other hands, has the advantage to show quantitatively the mean values and the distribution of defects and has some experimental advantages, for example, a wide temperature range and fast data collection. We present here results of LEED beam profile studies of O and H on Cu(110) at intermediate stages of the superstructure formation in order to observe the morphological changes caused by the reconstruction process.

Oxygen and hydrogen cause on the Cu(110) surface reconstructions of different type which both require mass transport of substrate atoms. Oxygen forms two ordered structures at different coverages, the (2 × 1) and the c(6 × 2) structure. The (2 × 1) structure has been studied with various methods including low energy ion scattering [1–3], LEED [4,5] helium diffraction [6], SEXAFS [7] and X-ray diffraction [8]. This list is not intended to be complete. There is now consensus reached about the structure which consists of Cu–O chains lying on top of a nearly undistorted substrate. Cu–O chains are also the main feature of the c(6 × 2) structure. For the latter structure additional Cu atoms are sitting above the chains keeping the chains together. This structure has been first determined by X-ray diffraction combined with ion scattering and STM studies [9] and could be well confirmed by a recent LEED study [10]. Both oxygen structures require mass trans-

port of substrate atoms. As has been shown by STM studies [11,12] the substrate atoms are dissolving at room temperature from the step edges and cause an observable shift of the steps. The structure is better described as an added row structure because the Cu–O chains are added to the substrate.

Hydrogen forms a (1×3) structure at temperatures below 150 K and a (1×2) structure in the temperature range between 160 and 320 K [13]. Only the (1×2) structure will be considered here. In an initial helium diffraction study the conclusion was drawn that the structure should form a buckled row model with subsurface hydrogen [14]. It could be shown later by ion scattering [15] that the (1×2) structure belongs to the missing row type reconstruction. This result could be well confirmed in the present LEED study [16]. Though hydrogen also forms a superstructure on Cu(110) which requires mass transport of Cu atoms the situation is slightly different to the case of oxygen adsorption. Oxygen builds up a composite layer containig O–Cu chains while hydrogen causes a reconstruction of the Cu(110) surface which becomes instable at a certain hydrogen coverage. In both cases the formation of the superstructure is an activated process.

The mechanism of the reconstruction after hydrogen adsorption is not well understood. The growth of reconstructed areas may start at step edges by diffusion of substrate atoms originating from kink sites. It is also possible that adsorbed hydrogen exceeding a critical density causes a rearrangement starting locally in small islands on the terraces. In the case of oxygen the STM results show that at room temperature Cu atoms desorb from steps causing a shift of step edges [11,12]. At higher temperatures creation of holes on the terraces occurs. In case holes are created this will be directly observable in the beam profiles by the oscillation of the widths of the specular beam as a function of the momentum transfer perpendicular to the surface.

To get more insight which terrace size and island arrangements are detectable and can be distinguished with a beam profile analysis we discuss first some possible models for a reconstruction process and the corresponding beam profiles. In sections 3 and 4 we present the results from beam profile measurements at intermediate stages of the reconstruction after oxygen and hydrogen adsorption. Results from both measurements will be discussed in section 5.

2. Diffraction from surfaces with steps and islands

The analysis of beam profiles diffracted from rough surfaces which are partially reconstructed requires a careful discussion which kind of defects become visible in the beam profile. The step distribution causes a broadening of the reflected beams which depends on the diffraction conditions. This is usually observed at the specular beam for convenience but the other beams exhibit a similar oscillation of the widths as well [17]. The finite size of the reconstructed islands causes an additional diffuse contribution to the beam profile. If the mean island size is much smaller than the terrace size the profile consists mainly of two diffuse components of Lorentzian shape which can be separated, in other cases when the different contributions cannot be separated a numerical analysis will be necessary to extract the information about the island and terrace sizes. The shape of the beam profile depends in general on the scattering factors of the different unit cells in reconstructed and non-reconstructed areas. To avoid a tedious calculation of the scattering factors it is convenient to investigate the widths of the beams as function of the phase difference between waves scattered in different levels, in the following denoted by $l = 2\pi/k_{\perp}d_{\perp}$. The discussion of beam profiles is based on the kinematic theory and is valid in the so called column approximation of the multiple scattering theory where multiple scattering effects at step edges or domain boundaries are neglected [18,19].

We may first remind the diffraction from clean statistically rough surfaces. The evaluation of the beam profiles has been described in several approaches. Usually a one-dimensional model is assumed with a geometric distribution of terrace sizes [19–22]. The resulting beam profiles are

Lorentzians and the analytic calculation is most convenient with the matrix method [19]. Having terraces and islands on the surface with different distributions the matrix method is practically not applicable. Therefore we have used here a new theoretical approach based on an extension of the matrix method which allows the calculation of beam profiles for arbitrary one-dimensional defect distributions [23]. Details of the calculation and a systematic investigation of beam profiles from partially reconstructed surfaces which are only qualitatively discussed here will be published elsewhere. We assume here that steps upwards and downwards occur with equal probability and that the surface is rough. The beam width then oscillates as a function of the momentum transfer perpendicular to the surface. The periodicity in reciprocal space defines the step height and the mean size follows from the maximum width at the "out of phase" diffraction condition ($l = 0.5$). This function is illustrated by the dashed line in fig. 1c.

We can distinguish three different cases schematically sketched in figs. 1–3. Case one corresponds to nucleation and growth of islands independent from the step structure. This case may occur at the deposition of material from an evaporation source. In the reconstruction process discussed here it corresponds to the case that the reconstruction nucleates at arbitrary points at the surface. The second case is given when the reconstruction nucleates only at steps. The material required for the growth of the reconstructed areas is supplied from uncovered steps. Only small changes of the mean terrace size will be observable in the beam profiles because the terraces can become smaller or larger. On an inclined surface with a step array a step flow mechanism will occur leaving the mean terrace size unchanged. At an intermediate stage where part of the surface is reconstructed we have the situation illustrated in fig. 2. A third case illustrated in fig. 3 occurs when the temperature is high enough that the creation of a vacancy/adatom pair on the terraces makes a relevant contribution to the source of substrate atoms. Then the creation of holes and new terraces will occur which now allows that reconstructed islands occur in levels different from the start configuration.

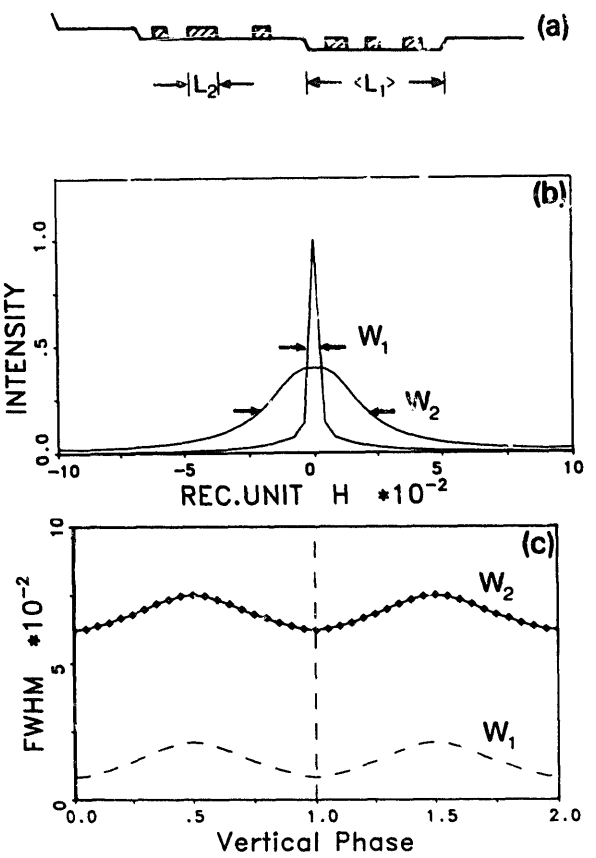

Fig. 1. (a) Statistical distribution of small reconstructed islands on large terraces. (b) The beam profiles consist of two Lorentzians, the narrow one corresponds to the mean terrace size $\langle L_1 \rangle$ and the broad one to the mean island size $\langle L_2 \rangle$ and the distance between islands as well. The relative height of the two Lorentzians depends on the structure factors and varies generally with the diffraction conditions. (c) The oscillation of the beam widths reflect the mean terrace size. Parameters: $\langle L_1 \rangle = 25$, $\langle L_2 \rangle = 5$, half coverage.

In the three cases discussed above the widths of the beam profiles exhibit a distinct dependency on the scattering vector. If adsorbate islands or reconstructed islands exist on the surface with a mean size much smaller than the mean terrace size then a broad diffuse profile occurs superposed to the narrower profile from the clean surface, see fig. 1b. We may assume that both contributions can be separated. The width of the diffuse profile remains broad at all diffraction conditions and oscillates only slightly as a function of the phase difference l (solid line in fig. 1c). It also appears a broad superstructure beam which reflects the average island size. The inte-

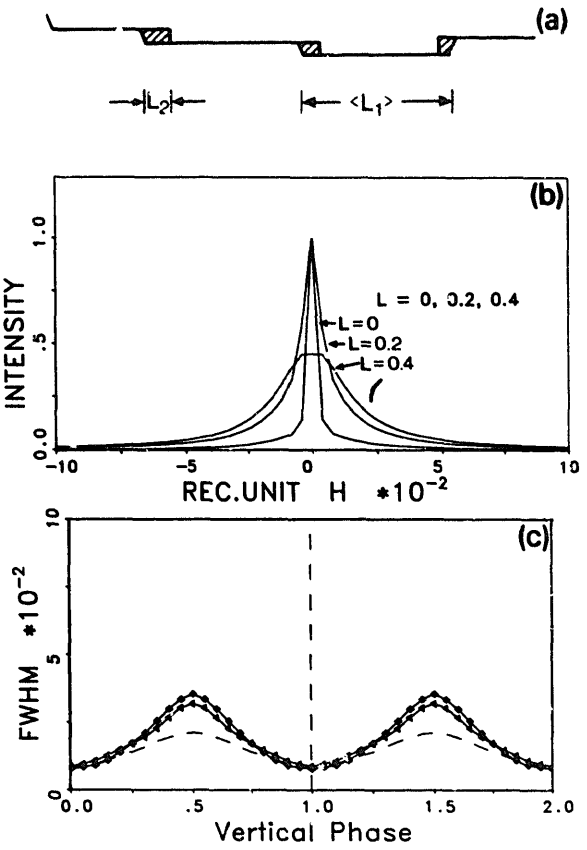

Fig. 2. (a) Schematic illustration of nucleation only at step edges. The distribution of reconstructed islands is strictly correlated to the distribution of steps. (b) Calculated beam profiles for $\langle L_1 \rangle = 25$ and $\langle L_2 \rangle = 5$ and half coverage. The profiles cannot be simply separated into two components. (c) The amplitude of the oscillation of the beam width of the partially reconstructed surface (solid lines) shows only a small increase compared to that of the clean surface (dashed line). The oscillation amplitude depends slightly on the relation between scattering factors, squares: $F_2/F_1 = 1.0$, triangles: $F_2/F_1 = 10.0$.

gral intensity of the superstructure beam is proportional to the reconstructed area.

The case illustrated in fig. 2 differs from the case in fig. 1 by the smaller number of reconstructed islands the distribution of which is now correlated to the step distribution. When nucleation only starts at steps the mean distance between islands is given by the mean terrace size of the unreconstructed surface. As a consequence the beam profiles cannot be separated into two contributions from different defect distributions and a numerical analysis of the profile will be necessary. The beam profile in general will not have a Lorentzian shape. The relative weight of different contributions to the profile depends on the relation between scattering factors. That the full width at half maximum (FWHM) in fig. 2 becomes small at the "in phase" diffraction condition $l = 0$ results from a broad foot of the profile which does not influence the FWHM. The main difference to fig. 1 is that the broad component is weaker and becomes narrower with increasing reconstructed area. The FWHM is only

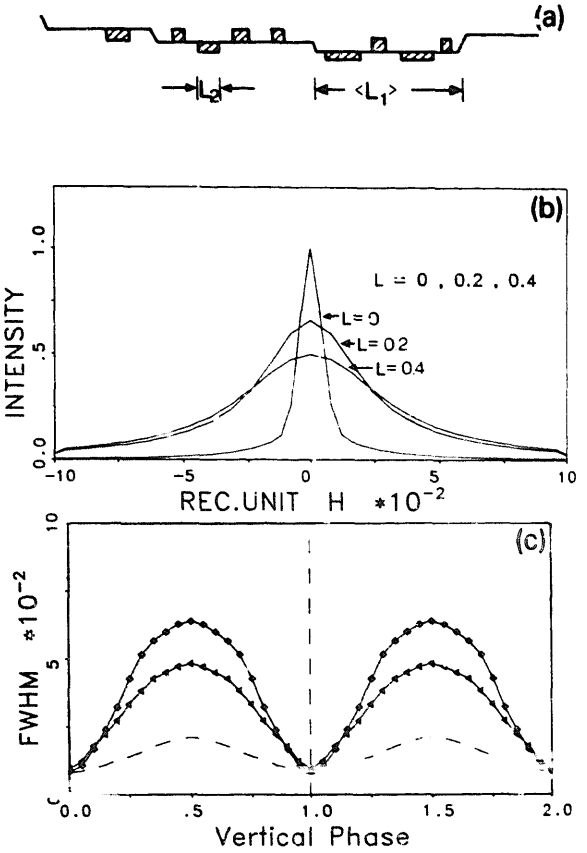

Fig. 3. (a) Model of the reconstruction where holes are created on the terraces. Reconstructed areas occur in different levels on a terrace. A statistical distribution of islands is assumed. (b) Calculated beam profiles for the parameters specified in fig 2. The beam profiles consist of two components which are not separated here. The shape deviates from a Lorentzian shape. (c) The oscillation amplitude (solid lines) has noticeably increased compared to that of the clean surface (dashed line). Its magnitude depends on the relation between scattering factors, squares: $F_2/F_1 = 1.0$, triangles $F_2/F_1 = 10.0$.

slightly increased at the "out of phase" diffraction condition.

A third case is given when atoms can be removed from terrace sites. This causes the creation of holes on the terraces and the ocurrence of reconstructed islands in different levels. In case the islands are much smaller than the terraces a bimodal distribution of terrace sizes occurs. The beam profiles consist of two components which both exhibit an oscillation of the width as a function of the phase difference. The profiles become much broader at $l = 0.5$ than in case 2 and the amplitude of the oscillation increases. This case is illustrated in fig. 3.

These different models discussed above represent limiting cases a mixture of which will occur in most cases. A clear interpretation of the beam profiles is in general only possible if the structure factors are known which requires a full dynamical calculation and the knowledge of the structures. However, from the observation of the beam widths (and possibly the beam shapes) as a function of the momentum transfer perpendicular to the surface the dominating process can be determined.

3. Oxygen adsorption on Cu(110)

The clean Cu(110) surface was prepared by sputtering and annealing at 600 K for 10–15 min. The angular profiles of the specular beam were measured with a Faraday cup. The mean terrace size of the clean surface was determined from the oscillation of the beam widths after deconvolution with the instrumental resolution function. The width of the instrumental function was determined from the minima of the width of the specular beam. Its shape was assumed to be Gaussian. The instrumental resolution determined in that way then includes all instrumental effects and the mosaic spread of the crystal as well. The mean terrace size was determined to about 120 Å. The resolution limit in a numerical analysis of the profiles is about 400 Å which was determined previously with a Ge crystal.

Oxygen was adsorbed at 150 K at a dosis of 0.5 to 2 L. The LEED pattern showed no signs of superstructures but the background increased.

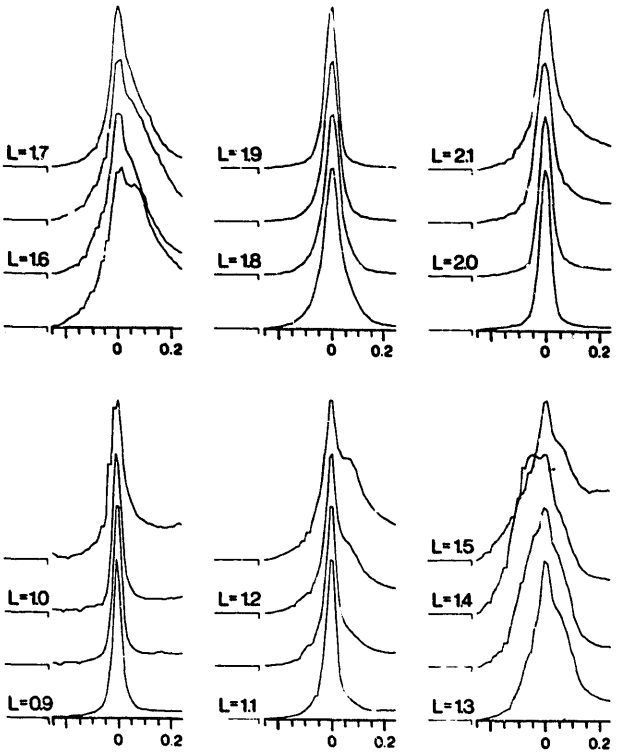

Fig. 4. Experimental (0,0)-beam profiles of oxygen covered Cu(110) surface after annealing at 300 K for 2 min O-exposure 0.5 L. The profiles are scaled to the same height. The profiles consist clearly of two components, the narrow component is nearly extinguished at $l = 1.5$, the broad component becomes narrow at $l = 1$ and 2. This indicates that mainly small reconstructed islands in different levels exist on the surface.

The crystal was subsequently annealed at 300 K for about 2 min. The diffraction pattern showed streaky half order beams and a significant increase of the width of the specular beam. Beam profiles are shown in fig. 4. The profiles consist obviously of two components, a broad and a narrow component. The width of the beam as a function of the phase difference l is shown in fig. 5. From the maximum width of the broad component we conclude a mean island size of about 15–20 Å. After annealing to 450 K for about 5 min the diffraction pattern exhibited sharp superstructure reflections and from the oscillation of the beam width we conclude a mean terrace size of about 120 Å. From the increase of the oscillation of the width after annealing at 300 K for 2 min it becomes obvious that the mean terrace size has become much smaller. The only possible

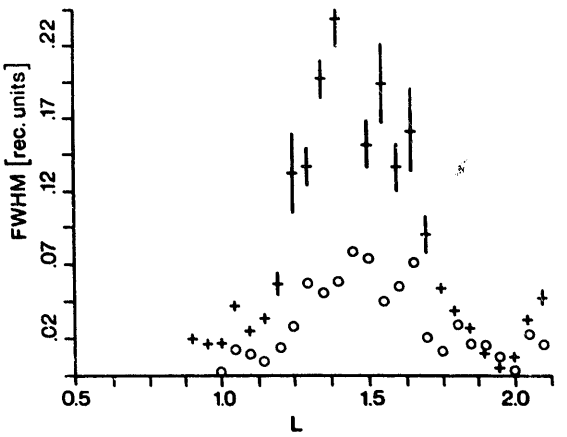

Fig. 5. Oscillation of the beam widths shown in fig. 4. after deconvolution with the instrumental resolution. The open circles show the beam widths of the clean surface before oxygen adsorption for comparison.

explanation for the large decrease of terrace sizes is the creation of new terraces and cannot be explained by a movement of steps alone.

However, a movement of steps by dissolving step atoms occurs as well. It can be concluded from the observation that the oscillation of the beam width after annealing showed double and quadruple periodicities indicating the existence of steps of up to 4 layer distances. Further observations are that the (0,0)-beam profile at lower oxygen coverages and annealing at 500 K exhibited satellites indicating the formation of (2×1) stripes as recently observed by helium diffraction [24] and STM studies [25]. The asperity height of the ordered (2×1) structure appeared to be smaller than that of the initially clean surface. A detailed discussion of the roughness and step height distribution will be discussed in a separate paper.

4. Hydrogen adsorption

Before performing beam profile measurements similar to that after oxygen adsorption we prepared a well ordered (1×2) structure of H/Cu(110) by adsorbing H at 150 K for about 40 min at 3×10^{-8} mbar and annealing at 300 K for about 5 min. The dose of atomic hydrogen cannot be specified. Hydrogen was dissociated by the hot filament of the mass spectrometer and the crystal was rotated to face the filament. The hydrogen exposure was repeated until a bright 1×2 pattern occurred. The width of the superstructure reflections appeared as narrow as the bulk beams.

Beam intensities were measured with a computer controlled video camera [26]. 14 symmetrically inequivalent beams at normal incidence were measured, each beam was averaged of 2 or 4 symmetrically equivalent ones. The LEED I/V analysis resulted in a clear preference for the missing row structure. In the analysis the two models which had been discussed previously have been considered, namely the buckled row model with hydrogen adsorbed above and below the top Cu layer [14] and the missing row model [15] with hydrogen adsorbed in different sites. The paired row model which had been found for H/Ni(110)-(1×2) [25] has been considered as well. In all models the possible relaxations in the uppermost three substrate layers compatible with the symmetry have been included. The R-factors for the final model are $R_{DE} = 0.31$, $R_P = 0.29$ and $R_{ZJ} = 0.14$. The corresponding r-factors for the other model were significantly worse. Details of the structure analysis will be published elsewhere [16].

The I/V analysis shows clearly the existence of the missing row model which requires mass diffusion over large distances. To observe the terrace widths during the reconstruction hydrogen was adsorbed at 150 K and the crystal was annealed in several steps starting at 200 K and subsequently increasing the temperature until at 320 K hydrogen was desorbed. The beam profiles were measured with the video camera and are therefore more noisy than the measurements with the Faraday cup. The measurement with the video system had also the consequence that the specular beam could not be measured because of the reflected light from the cathode of the electron gun. Therefore the profiles of the (0,1) and (0,1.5) beams were measured. The beam profiles at intermediate stages are shown in fig. 6. The formation of the (1×2) structure is monitored by the (0,1.5) beam. Up to 250 K no indication for the (1×2) structure is found. The (0,1.5) beam appears after 1 min annealing at 283 K, reaches a maximum after about 7 min annealing at this

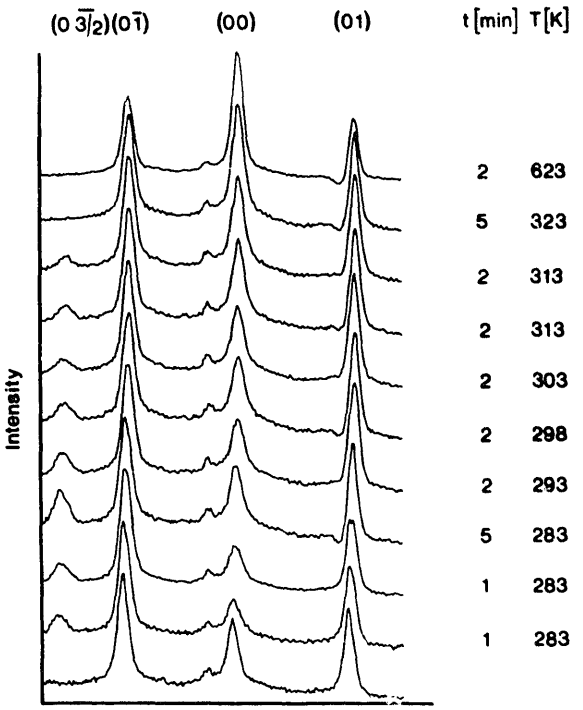

Fig. 6. Sequence of profiles of beams after hydrogen adsorption at 130 K and subsequent annealing at temperatures indicated in the figure. The small peak at the left side of the (0,0)-beam is an optical reflection from the electron gun.

temperature and has completely disappeared at 320 K.

There is no significant broadening of the (0,1) beam visible. The width of the half order beam remains nearly constant. This means the mean size of the reconstructed islands exceeds the transfer width of the LEED system even in the initial stages when only a small fraction of the surface is reconstructed. This corresponds to the observation that no significant broadening of the (0,1)-beam can be detected. This is the case for the reconstruction process as well as for the deconstruction process above 300 K when hydrogen starts to desorb.

5. Discussion

The beam profiles after oxygen adsorption show clearly an increase of the step density. According to the model calculations described above this can only be caused by a creation of holes on the terraces. This result is consistent with the picture of the growth process determined in recent STM investigations of the growth mechanism [26,27] and also in an ICISS study [28]. In the early stage of the reconstruction a mobile oxygen layer traps the Cu adatoms evaporating from steps. In the later stages the creation of holes becomes competitive. After 2 min annealing at 300 K (2 × 1) islands of about 15–20 Å diameter in (001) direction are formed. At this stage nearly the whole surface is covered with (2 × 1) islands as becomes obvious in the beam profile at the "out of phase" diffraction condition. The narrow component of the beam profile is nearly extinguished. As has been seen in the STM pictures [28] the steps are stabilised by the (2 × 1) structure and the migration of adatoms over the (2 × 1) islands is slowed down which means that the supply of adatoms is restricted. Further growth of (2 × 1) islands proceeds via creation of holes.

The mechanism of the reconstruction after hydrogen adsorption is obviously different. There is no increase of the step density visible. This observation makes it unlikely that the formation of the (1 × 2) structure proceeds via the creation of holes on the terraces. The surface is only partially reconstructed after 2 min annealing at 273 K, further growth needs a supply of Cu atoms, or a sink for Cu atoms respectively. This obviously does not take place by further nucleation on the terraces but by growth of the (1 × 2) islands. The difference to the oxygen (2 × 1) structure may have the reason that the diffusion of Cu adatoms is not significantly hindered in the (1 × 2) structure and that the production of adatoms by evaporation from steps, or the sticking of adatoms at the steps, is not suppressed by (1 × 2) islands. It follows that the kinetics of the (1 × 2) reconstruction should be different from that of the formation of the (2 × 1) structure. A detailed analysis of the beam profiles and the kinetics of the system is in preparation. We conclude here that the missing row reconstruction most probably starts with nucleation at steps and that the growth of the (1 × 2) islands proceeds by migration of steps.

Acknowledgements

Stimulating discussions with Professor R.J. Behm are gratefully acknowledged. This work was financially supported by the Deutsche Forschungsgemeinschaft, SFB 338.

References

[1] H. Niehus and G. Comsa, Surf. Sci. 140 (1984) 18.
[2] E. van de Riet, J.B.J. Smeets, J.M. Fluit and A. Niehaus, Surf. Sci. 214 (1989) 111.
[3] H. Dürr, Th. Fauster and R. Schneider, Surf. Sci. 244 (1991) 237.
[4] S.R. Parkin, H.C. Zheng, M.Y. Zhou and K.A.R. Mitchell, Phys. Rev. B 41 (1990) 5432.
[5] J. Wever, J. Zueter, R. Zuschke, D. Wolf and W. Moritz, to be published.
[6] J. Lapujoulade, Y. Le Cruër, M. Lefort, Y. Lejay and E. Maurel, Surf. Sci. 118 (1982) 103.
[7] M. Bader, A. Puschmann, C. Ocal and J. Haase, Phys. Rev. Lett. 57 (1986) 3273.
[8] R. Feidenhans'l, F. Grey, R.L. Johnson, S.G.J. Mochrie, J. Bohr and M. Nielsen, Phys. Rev. B 41 (1990) 5420.
[9] R. Feidenhans'l, F. Grey, M. Nielsen, F. Besenbacher, F. Jensen, E. Laesgaard, I. Stensgaard, K.W. Jacobsen, I.K. Nørskov and R.L. Johnson, Phys. Rev. Lett. 65 (1990) 2027.
[10] R. Zuschke, Zi Pu Hu, D. Wolf and W. Moritz, to be published.
[11] D.J. Coulman, J. Wintterlin, R.J. Behm and G. Ertl, Phys. Rev. Lett. 64 (1990) 1761.
[12] F. Jensen, F. Besenbacher, E. Laesgaard and I. Stensgaard, Phys. Rev. B 41 (1990) 10233.
[13] S. Engel, M. Horn and K. Christmann, to be published.
[14] K.H. Rieder and W. Stocker, Phys. Rev. Lett. 57 (1986) 2548.
[15] R. Spitzl, H. Niehus, B. Poelsema and G. Comsa, Surf. Sci. 239 (1990) 243.
[16] R. Zuschke, W.Moritz and D. Wolf, to be published.
[17] M. Henzler, Appl. Surf. Sci. 11/12 (1982) 450.
[18] W. Moritz, in: Reflection High Energy Electron Diffraction and Reflection Electron Imaging of Surfaces (Plenum, New York, 1988) p. 175.
[19] H. Jagodzinski, W. Moritz and D. Wolf, Surf. Sci. 77 (1978) 233.
[20] C.S. Lent and P.I. Cohen, Surf. Sci. 139 (1984) 121.
[21] T.M. Lu and M.G. Lagally, Surf. Sci. 120 (1982) 47.
[22] For a review see: M.G. Lagally, D.E. Savage and M.C. Tringides, in: Reflection High Energy Electron Diffraction and Reflection Electron Imaging of Surfaces (Plenum, New York, 1988) p. 139.
[23] S. Pflanz and W. Moritz, Acta Cryst., in press.
[24] K. Kern, H. Niehus, A. Schatz, P. Zeppenfeld, J. Goerge and G. Comsa, Phys. Rev. Lett. 67 (1991) 855.
[25] G. Kleinle, V. Penka, R.J. Behm, G. Ertl and W. Moritz, Phys. Rev. Lett. 58 (1987) 148.
[26] J. Wintterlin, R. Schuster, D.J. Coulman and G. Ertl, Surf. Sci., in press.
[27] F. Besenbacher, I. Stensgaard, L. Ruan, J.K. Norskov and K.W. Jacobsen, Surf. Sci. 272 (1992) 334.
[28] H. Dürr, R. Schneider and Th. Fauster, Phys. Rev. B, in press.